

Spin Polarization and Anomalous Magnetic Moment in a (2 + 1)-flavor Nambu-Jona-Lasinio model in the thermomagnetic background

Yi-Wei Qiu¹ and Sheng-Qin Feng^{1,2,3,*}

¹*College of Science, China Three Gorges University, Yichang 443002, China*

²*Key Laboratory of Quark and Lepton Physics (MOE) and Institute of Particle Physics, Central China Normal University, Wuhan 430079, China*

³*Center for Astronomy and Space Sciences, China Three Gorges University, Yichang 443002, China*

(Dated: January 5, 2023)

Abstract

Abstract: We investigate the magnetized QCD matter and chiral phase transition in a (2 + 1)-flavor Nambu–Jona-Lasinio (NJL) model at finite temperature and chemical potential by comparing the contributions from the tensor spin polarization (TSP) and anomalous magnetic moment (AMM) of quarks. For light u and d quarks, when TSP and AMM are not considered, the magnetized system is characterized by magnetic catalysis. The introduction of TSP will further enhance the magnetic catalytic characteristics. On the other hands, when AMM is introduced, the phase transition temperature decreases with the magnetic field, which is the feature of inverse magnetic catalysis. The phase diagram of u and d quarks will change from the crossover phase transition to the first order phase transition with the increase of magnetic field and chemical potential when AMM is induced. The phase diagram will not change from the crossover phase transition to the first order phase transition when TSP is induced. For the phase diagram of strange s quark, whether TSP or AMM is induced, the phase diagram will keep a crossover phase transition with the increase of magnetic field and chemical potential.

* Corresponding author: fengsq@ctgu.edu.cn

I. INTRODUCTION

Comprehending properties of QCD matter under a strong magnetic field is of essential importance to further investigate the evolution of the early universe [1], non-central heavy-ion collisions [2–5], neutron-star merges [6, 7], and the interior of magnetar [8, 9]. The exploration of the QCD vacuum and strongly interacting matter under external strong magnetic fields has fascinated much attention, see reviews, e.g., Refs. [10–14]. Here we stress the study of the magnetic field of non-central heavy-ion collisions, which comes from the laboratory of mankind. The magnetic field reaches up to $\sqrt{eB} \sim 0.1\text{GeV}$ for RHIC and $\sqrt{eB} \sim 0.5\text{ GeV}$ for LHC in non-central heavy-ion collisions. This magnetic field is external since it is generated by the spectators, and though it has a very short lifetime (of the order of $1\text{ fm}/c$). However, as taken in Refs. [15–18], the presence of the quark-gluon plasma (QGP) medium response effect, substantially delays the decay of these time-dependent magnetic fields. This is why in the most cases, the effect of constant and uniform magnetic fields on quark matter is discussed in the literature. The magnetic field coincides with the production of the QGP and thus may have a fairly important effect on the properties of the phase transition. For example, the chiral magnetic effect (CME) [16, 19–22], magnetic catalysis (MC) in the vacuum [23–25], inverse magnetic catalysis (IMC) around the chiral phase transition [26–29].

The magnetic field can lead to spin polarization, that is, the condensation of quark anti-quark ($\bar{q}q$) pairs with spin parallel. Ref.[30] shows that a tensor-type interaction $\sim (\bar{\psi}\Sigma^3\psi)^2 + (\bar{\psi}i\gamma^5\Sigma^3\psi)^2$ produces a spin polarization (SP) $\langle\bar{\psi}i\gamma^1\gamma^2\psi\rangle$, which is very similar to the anomalous magnetic moment (AMM) produced by quarks in a magnetic field. The tensor polarization operator $\bar{\psi}\sigma^{\mu\nu}\psi$ can also be named as the spin polarization operator, or the spin density since $\bar{\psi}\sigma^{12}\psi = \psi\gamma^0\Sigma^3\psi$. If the quark spinor ψ is projected into the sub-spin space $\psi = \psi_{\uparrow} + \psi_{\downarrow}$, corresponding to $\bar{\psi}\sigma^{12}\psi \sim \langle\bar{\psi}_{\uparrow}\psi_{\uparrow}\rangle - \langle\bar{\psi}_{\downarrow}\psi_{\downarrow}\rangle$, which can be used to measure the difference between the spin-up quark pair and the spin-down quark pair.

We investigate the magnetized QCD matter in a $(2 + 1)$ -flavor Nambu–Jona-Lasinio (NJL) model at finite temperature and chemical potential by comparing the contributions from the tensor spin polarization (TSP) and AMM of quarks. For a particle with charge e , mass m and spin \vec{s} , its corresponding magnetic moment (MM) is μ . Corresponding to $\bar{q}q$ pair with antiparallel spin pairs, it has a net magnetic moment (MM), so the chiral

condensation triggers a dynamic AMM. Under the action of the magnetic field, the net MM tends to be parallel to the magnetic field. For SP with $\bar{q}q$ pair parallel spin pairing, the MM of spin-aligned quarks and anti-quarks cancel each other, and the spin polarization pairing does not present a net MM. Therefore, compared with the chiral condensation with a nonzero net MM, the total MM of the system considering SP condensation will reduce. Therefore, systems with spin polarization are expected to exhibit relative diamagnetism. At high temperatures, the pair of $\bar{q}q$ dissociates, and all charged quarks become a single small magnet, which is arranged in turn along the magnetic field; Therefore, QCD matter at high temperature manifests paramagnetism.

The catalysis of chiral symmetry breaking induced by a magnetic field, namely the MC effect, can be easily understood from dimension reduction. On the other hand, IMC effect, the critical temperature of the chiral phase transition decreases with the increasing magnetic field, which is intuitively contradictory to the MC effect and is still a puzzle. Although there are many publications trying to explain IMC by considering running coupling constant generated by the magnetic field [31] and chiral imbalance caused by sphaleron transition or instanton anti-instanton pairing [32]. Some interesting and novel properties of magnetized QCD materials have recently been presented by lattice calculations, for example, magnetized materials exhibit paramagnetism (positive susceptibility) at high temperatures and diamagnetism (negative susceptibility) at low temperatures [33, 34].

The effect of an AMM of quark has drawn quite a lot of interest recently [35–41] in order to investigate the IMC effect. The dynamical chiral symmetry broken is known as one of the most important characteristics of QCD, which makes quarks achieve a dynamical mass of QCD. Refs. [42, 43] pointed out that quarks' AMM can also be dynamically produced like the dynamic quark mass. Therefore, once quarks achieve dynamic mass, they should also achieve dynamical AMM [42, 44–46]. The coefficient κ of quarks' AMM in the magnetic field by the effective interaction $\frac{1}{2}q\kappa F_{\mu\nu}\bar{\psi}\sigma^{\mu\nu}\psi = \frac{1}{2}[\gamma^\mu, \gamma^\nu]$ is introduced and the IMC effect at finite temperature is proposed by Ref. [47]. For QCD, both explicit and spontaneous chiral symmetry breaking is dedicated to the AMM of quarks, which is also called dynamical AMM [43].

In this paper, we investigate the magnetism of QCD matter and chiral phase transition under a magnetic field with the contribution from the TSP and the AMM of quarks respectively. This paper is organized as follows: in Sec. II, we introduce the (2 + 1)-flavor

NJL models by including the AMM and the TSP in the external magnetic field respectively. In Sec. III, we investigate MC and IMC by the AMM and TSP, respectively. Then the dependencies of dynamical mass, entropy, sound-velocity, and critical point on the magnetic field by comparing the contributions from the TSP and the AMM of quarks are studied in Sec. III. Finally, we make the summaries and conclusions in Sec. IV.

II. THE 2 + 1 FLAVORS NJL MODEL UNDER A MAGNETIC FIELD

The Lagrangian density of the (2 + 1)-flavor NJL model [48, 49] in the presence of an external magnetic field is given as:

$$\begin{aligned} \mathcal{L} = & \bar{\psi} (i\gamma^\mu D_\mu + \gamma^0 \mu - m) \psi + G_s \sum_{a=0}^8 \left[(\bar{\psi} \lambda_a \psi)^2 + (\bar{\psi} i\gamma^5 \lambda_a \psi)^2 \right] \\ & - K \left[\det \bar{\psi} (1 + \gamma_5) \psi + \det \bar{\psi} (1 - \gamma_5) \psi \right], \end{aligned} \quad (1)$$

where the quark field ψ carries three flavors ($f = u, d, s$) and three colors ($c = r, g, b$), and $\lambda_a (a = 1, \dots, N_f^2 - 1)$ represents the SU(3) Gell-Mann matrices in the three flavor space. Current quark mass m is considered as $m_u = m_d$ for isospin symmetry of light quarks, strange quark mass m_s is different from the other light quark (m_u and m_d) masses. The difference between the strange and non-strange quark masses obviously breaks the SU(3) flavor symmetry. μ is the quark chemical potential, and we assume that the quark chemical potentials of the strange and non-strange quarks are the same. A covariant derivative with magnetic field is introduced as $D_u = \partial_\mu + iQA_\mu^{\text{ext}}$, and the charge matrix in flavor space is

$$Q = \text{diag}(q_u, q_d, q_s) = \text{diag}\left(\frac{2}{3}, -\frac{1}{3}, -\frac{1}{3}\right). \quad (2)$$

In general, if one chooses the gauge field $A_\mu^{\text{ext}} = (0, 0, Bx_1, 0)$, a constant magnetic field should point at the x^3 -direction. The K term of Eq. (1) is the term of Kobayashi-Maskawa-t'Hooft interaction [49–51].

A. The introduction of a (2 + 1)- flavors NJL model with TSP

It is shown that [30, 35] the breaking of the rotational symmetry by a uniform magnetic field induces a separation between longitudinal and transverse fermion modes along the direction of the magnetic field. This separation gives rise to the effective splitting of the

couplings in the one-gluon exchange interactions on which the NJL models are usually based. This splitting is therefore reported in the four-fermion couplings of a QCD-inspired NJL model in a magnetic field, and we can use the Fierz identities in a magnetic field [30, 31, 52] to propose the interactions of scalar and tensor of the (2 + 1)-flavor NJL Lagrangian:

$$\begin{aligned} \mathcal{L}_{\text{TSP}} = & \bar{\psi} (i\gamma^\mu D_\mu + \gamma^0 \mu - m) \psi + G_s \sum_{a=0}^8 \left[(\bar{\psi} \lambda_a \psi)^2 + (\bar{\psi} i\gamma^5 \lambda_a \psi)^2 \right] + G_t \sum_{a=0}^8 \\ & \left\{ (\bar{\psi} \Sigma_3 \lambda_a \psi)^2 + (\bar{\psi} \Sigma_3 i\gamma^5 \lambda_a \psi)^2 \right\} - K \left\{ \det [\bar{\psi} (1 + \gamma_5) \psi] + \det [\bar{\psi} (1 - \gamma_5) \psi] \right\}. \end{aligned} \quad (3)$$

The coupling constant G_s in the scalar/pseudo-scalar channel is closely related to the spontaneously chiral symmetry breaking, which produces a dynamical quark mass, and the tensor/ pseudo-tensor channels term $G_t \sum_{a=0}^8 \left[(\bar{\psi}_f^c \Sigma^3 \lambda_a \psi_f^c)^2 + (\bar{\psi}_f^c i\Sigma^3 \gamma^5 \lambda_a \psi_f^c)^2 \right]$ is closely related to the spin-spin interaction, which causes spin polarization condensation.

For the (2 + 1)-flavor NJL model, tensor-type interaction at the mean field level leads to two types of spin polarization as

$$\begin{aligned} F_3 &= -2G_t \langle \bar{\psi} \Sigma^3 \lambda_3 \psi \rangle, \\ F_8 &= -2G_t \langle \bar{\psi} \Sigma^3 \lambda_8 \psi \rangle. \end{aligned} \quad (4)$$

In general, F_3 contains only u and d quark spin polarization condensates, on the other hand, F_8 is associated with the strange quark spin polarization condensate. The running coupling constants are divided into longitudinal (g_{\parallel}) and transverse (g_{\perp}) components due to the existence of the magnetic field. In our current study, the couplings of the above NJL interactions relevant to quark gluon vertex coupling are expressed as $G_s = (g_{\parallel}^2 + g_{\perp}^2) / \Lambda^2$ and $G_t = (g_{\parallel}^2 - g_{\perp}^2) / \Lambda^2$. The distinguishing transverse and parallel Fierz identities automatically create a new channel of four-fermion interaction term with second order tensor structure in Lagrangian density during the transformation from splitting quark-gluon coupling to the scalar and pseudoscalar bilinear quantity [30]. G_s and G_t can be considered as the scalar and tensor channel interaction couplings, respectively.

The effective potential by using standardized process is given

$$\begin{aligned}
\Omega_{\text{TSP}} = & G_s \sum_{f=u,d,s} \langle \bar{\psi} \psi \rangle_f^2 + G_t \langle \bar{\psi} \lambda_3 \Sigma^3 \psi \rangle^2 + G_t \langle \bar{\psi} \lambda_8 \Sigma^3 \psi \rangle^2 - \frac{N_c}{2\pi} \sum_{f=u,d,s} |q_f B| \sum_{l=0}^{\infty} \alpha_l \int_{-\infty}^{\infty} \frac{dp_z}{2\pi} \\
& \times \left\{ \varepsilon_{f,l,\eta} + T \ln \left[1 + \exp \left(\frac{-\varepsilon_{f,l,\eta} - \mu}{T} \right) \right] + T \ln \left[1 + \exp \left(\frac{-\varepsilon_{f,l,\eta} + \mu}{T} \right) \right] \right\} \\
& + 4K \langle \bar{\psi} \psi \rangle_u \langle \bar{\psi} \psi \rangle_d \langle \bar{\psi} \psi \rangle_s
\end{aligned} \tag{5}$$

where $l = 0, 1, 2 \dots$ represents the quantum number of Landau level, and $\eta = \pm 1$ corresponds to the two kinds of spin direction of quark-antiquark ($\bar{q}q$) pair. Contribution of non-degenerate particles due to spin difference at non-lowest Landau energy levels can be taken into account with the definition of this new operator $\alpha_l = \delta_{0,l} + \Delta(l) \sum_{\eta=\pm 1}$, where $\Delta(l)$ is denoted by

$$\Delta(l) = \begin{cases} 0 & l = 0 \\ 1 & l > 0 \end{cases} \tag{6}$$

and the energy spectrum of the lowest Landau Level (LLL) ($l = 0$) and non-LLL ($l \neq 0$) are given as

$$\begin{aligned}
\varepsilon_{u,l=0}^2 &= p_z^2 + \left(M_f + \left(F_3 + \frac{F_8}{\sqrt{3}} \right) \right)^2, \\
\varepsilon_{u,l \neq 0, \eta = \pm 1}^2 &= p_z^2 + \left(\sqrt{M_f^2 + 2|q_f B|l} + \eta \left(F_3 + \frac{F_8}{\sqrt{3}} \right) \right)^2, \\
\varepsilon_{d,l=0}^2 &= p_z^2 + \left(M_f + \left(F_3 - \frac{F_8}{\sqrt{3}} \right) \right)^2, \\
\varepsilon_{d,l \neq 0, \eta = \pm 1}^2 &= p_z^2 + \left(\sqrt{M_f^2 + 2|q_f B|l} + \eta \left(F_3 - \frac{F_8}{\sqrt{3}} \right) \right)^2, \\
\varepsilon_{s,l=0}^2 &= p_z^2 + \left(M_f + \left(\frac{2F_8}{\sqrt{3}} \right) \right)^2, \\
\varepsilon_{s,l \neq 0, \eta = \pm 1}^2 &= p_z^2 + \left(\sqrt{M_f^2 + 2|q_f B|l} + \eta \left(\frac{2F_8}{\sqrt{3}} \right) \right)^2.
\end{aligned} \tag{7}$$

Note that the breaking of energy spectrum degeneracy caused by spin known as Zeeman effect. Therefore, the contributions of spin come not only from the ground state of Landau level, but also from the whole excited states of Landau level. The tensor condensate parameter F_3 and F_8 are self-consistently satisfied the minimum of the thermodynamic potential,

which are similar to dynamical quark mass M_f . At first, one can obtain three gap equations for M_f ($f = u, d, s$)

$$\frac{\partial \Omega_{\text{TSP}}(M_f, F_3, F_8)}{\partial M_f} = 0, \quad (8)$$

and the other two gap equations for F_3 and F_8 is given as

$$\begin{aligned} \frac{\partial \Omega_{\text{TSP}}(M_f, F_3, F_8)}{\partial F_3} &= 0, \\ \frac{\partial \Omega_{\text{TSP}}(M_f, F_3, F_8)}{\partial F_8} &= 0. \end{aligned} \quad (9)$$

To ensure that the thermodynamic potential in vacuum returns to zero, we define the normalized thermodynamic potential as effective potential

$$\Omega_{\text{eff}}(T, \mu, eB) = \Omega(T, \mu, eB) - \Omega(0, 0, eB). \quad (10)$$

Some of the relevant thermodynamical quantities can be evaluated by the effective potential. The quark number density is

$$\rho_f = \sum_{l, \eta} \frac{N_c |q_f eB|}{4\pi^2} \int_{-\infty}^{\infty} dp_z (n^+ - n^-), \quad (11)$$

where $n^\pm = 1/(\exp[(\varepsilon_{f,l,\eta} \mp \mu)/T] + 1)$ is quark (antiquark) number distribution. The entropy density $S_f = -\frac{\partial \Omega_{\text{eff}}}{\partial T}$ is given as

$$S_f = - \sum_{l, \eta} \frac{N_c |q_f eB|}{4\pi^2} \int_{-\infty}^{\infty} dp_z \left[\ln(1 - n^+) + \ln(1 - n^-) - \frac{\varepsilon_{f,l,\eta}}{T} (n^+ + n^-) + \frac{\mu}{T} (n^+ - n^-) \right]. \quad (12)$$

The energy density is given as

$$\varepsilon = T \frac{\partial P}{\partial T} + \mu \frac{\partial P}{\partial \mu} - P, \quad (13)$$

where P is pressure. The square of sound-speed are defined as

$$c_s^2 = \frac{\partial P}{\partial \varepsilon} = \left(\frac{\mu}{S_f} \frac{\partial \rho_f}{\partial T} + \frac{T}{S_f} \frac{\partial S_f}{\partial T} \right)^{-1}. \quad (14)$$

B. the introduction of the (2 + 1)- flavor NJL model with AMM

The effective Lagrangian density of the (2 + 1)- flavor with AMM [48, 49] is given as

$$\begin{aligned} \mathcal{L}_{\text{AMM}} = & \bar{\psi} \left(i\gamma^\mu D_\mu + \gamma^0 \mu - m + \frac{1}{2} q_f \kappa \sigma^{\mu\nu} F_{\mu\nu} \right) \psi \\ & + G_s \sum_{a=0}^8 \left[(\bar{\psi} \lambda_a \psi)^2 + (\bar{\psi} i\gamma^5 \lambda_a \psi)^2 \right] - K \left[\det \bar{\psi} (1 + \gamma_5) \psi + \det \bar{\psi} (1 - \gamma_5) \psi \right]. \end{aligned} \quad (15)$$

The effective potential with AMM can be taken as

$$\begin{aligned} \Omega_{\text{AMM}} = & G_s \sum_{f=u,d,s} \langle \bar{\psi} \psi \rangle_f^2 + 4K \langle \bar{\psi} \psi \rangle_u \langle \bar{\psi} \psi \rangle_d \langle \bar{\psi} \psi \rangle_s - \frac{N_c}{2\pi} \sum_{f=u,d,s} |q_f B| \sum_{l=0}^{\infty} \sum_{t=\pm 1} \int_{-\infty}^{\infty} \frac{dp_z}{2\pi} \\ & \times \left\{ E_{f,l,t} + T \ln \left[1 + \exp \left(\frac{-E_{f,l,t} - \mu}{T} \right) \right] + T \ln \left[1 + \exp \left(\frac{-E_{f,l,t} + \mu}{T} \right) \right] \right\}, \end{aligned} \quad (16)$$

where

$$E_{f,l,t} = \sqrt{p_z^2 + \left((M_f^2 + 2|q_f B|l)^{1/2} - t\kappa_f q_f eB \right)^2} \quad (17)$$

is the energy spectrum under different Landau energy levels, and $t = \pm 1$ corresponds to the two kinds of spin direction of $\bar{q}q$ pair. One can obtain three coupling gap equations for each order parameter as

$$\frac{\partial \Omega_{\text{AMM}}}{\partial M_f} = 0, \quad (18)$$

where $f = u, d, s$ for the three different flavors. Thus we can obtain three dynamical quark masses of $u, d,$ and s as

$$\begin{aligned} M_u &= m_u - 4G_s \langle \bar{\psi} \psi \rangle_u + 2K \langle \bar{\psi} \psi \rangle_d \langle \bar{\psi} \psi \rangle_s, \\ M_d &= m_d - 4G_s \langle \bar{\psi} \psi \rangle_d + 2K \langle \bar{\psi} \psi \rangle_u \langle \bar{\psi} \psi \rangle_s, \\ M_s &= m_s - 4G_s \langle \bar{\psi} \psi \rangle_s + 2K \langle \bar{\psi} \psi \rangle_u \langle \bar{\psi} \psi \rangle_d, \end{aligned} \quad (19)$$

where

$$\langle \bar{\psi} \psi \rangle_f = \frac{N_c G_s}{2\pi} \sum_{l=0}^{\infty} \alpha_l |q_f B| \int_{-\infty}^{+\infty} \frac{dp_z}{2\pi} \frac{M_f}{\varepsilon_{f,l,t}} \left(1 - \frac{s\kappa_f q_f B}{\hat{M}_{f,l,t}} \right) \left\{ 1 - \frac{1}{e^{\frac{\varepsilon_{f,l,t} + \mu}{T}} + 1} - \frac{1}{e^{\frac{\varepsilon_{f,l,t} - \mu}{T}} + 1} \right\} \quad (20)$$

corresponds to chiral condensation of different quark flavors.

III. RESULTS AND DISCUSSIONS

To calibrate sets of parameters to applicable observable, parameters are referred [49, 53] to be chosen as: $\Lambda = 631.4$ MeV, $m_u = m_d = 5.6$ MeV, $m_s = 135.7$ MeV, $\Lambda^2 G_s = 1.835$ and $K\Lambda^5 = 9.29$. The empirical values are given as $f_\pi = 93$ MeV, $m_\pi = 138$ MeV, $m_K = 495.7$ MeV, and $m_{\eta'} = 957.5$ MeV.

The tensor channel coupling constant G_t restricted by the magnetic fields ought to be zero in the case of the vanished magnetic field, and equals the value of G_s when $eB \rightarrow \infty$. At the following study, the value of G_t is taken as $G_t = G_s/2$.

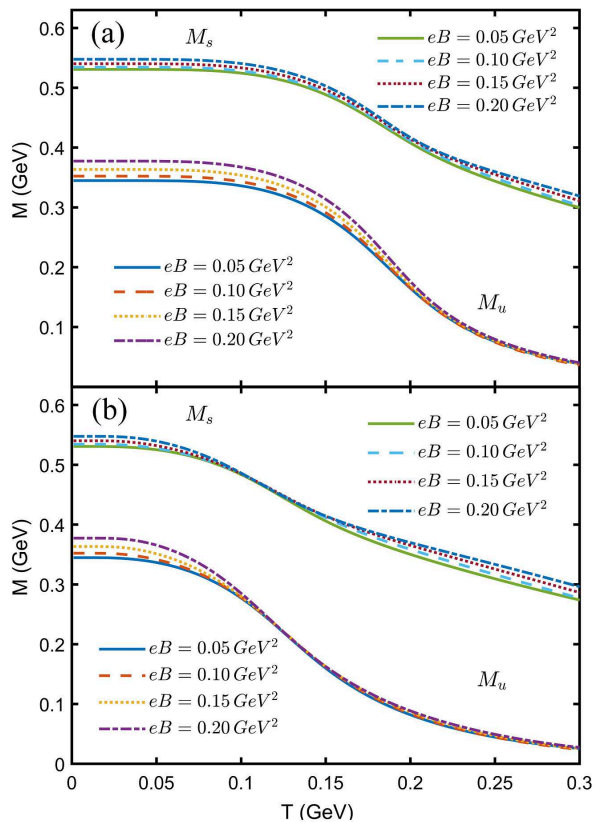


FIG. 1. The dependence of dynamical quark mass (M) on temperature (T) for four different magnetic fields ($eB = 0.05, 0.10, 0.15$ and 0.20 GeV^2), which does not consider TSP and AMM. Fig 1.(a) is for $\mu = 0.0$ GeV; and Fig 1.(b) is for $\mu = 0.25$ GeV.

In order to investigate the effect of AMM on the phase transition, we make comparisons between the two AMM sets. The compatible results obtained in [54] we define it as AMM1 set as $\kappa_u = \kappa_d = 0.38$, $\kappa_s = 0.25$, while the defined AMM2 set chosen as $\kappa_u = 0.123$, $\kappa_d =$

0.555, $\kappa_s = 0.329$ fixed by [55].

Due to the NJL model is non-renormalizable, the divergent vacuum terms merged in gap equation regularized by using the magnetic-field-independent regularization (MIFR) scheme [56, 57], which gets rid of the nonphysical part by separating the vacuum term from the integrals. The scheme dealing with the sums of all Landau level within the integrals by means of Hurwitz zeta function are presented.

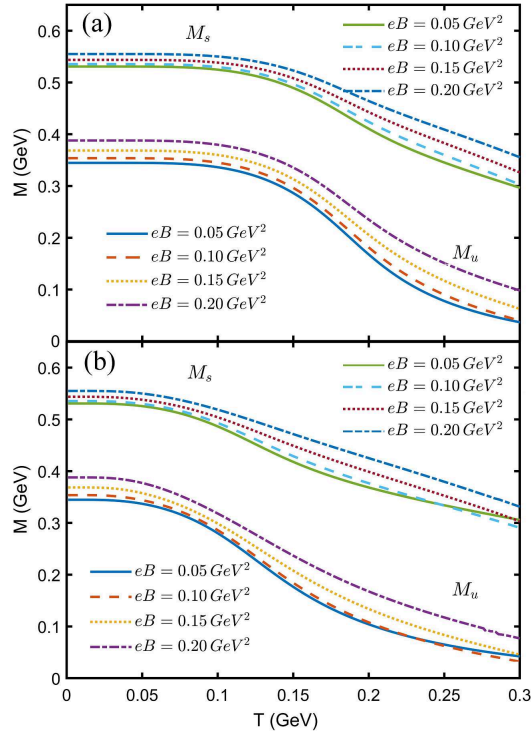


FIG. 2. The dependence of dynamical quark mass (M) on temperature (T) for four different magnetic fields ($eB = 0.05, 0.10, 0.15$ and 0.20 GeV^2) by considering TSP. Fig 2.(a) is for $\mu = 0.0 \text{ GeV}$; and Fig 2.(b) is for $\mu = 0.25 \text{ GeV}$.

The dynamical mass or the quark condensate plays as an order parameter for the chiral phase transition. Chiral restoration happens at high temperatures and/or high chemical potentials. In Fig. 1(a, b), the dynamical quark masses M of u , d and s quarks without considering AMM and TSP are manifested as decreasing smooth functions of temperatures at $\mu = 0$ and $\mu = 0.25 \text{ GeV}$, which indicates a chiral crossover. The dynamical mass M is apparently enhanced by increasing the magnetic field. The magnetic field is shown at $eB = 0.05, 0.1, 0.15$, and 0.2 GeV^2 with $\mu = 0$ and $\mu = 0.25 \text{ GeV}$ respectively. Since we

have considered non-vanishing current quark mass, the chiral symmetry is never restored fully. Since the dynamical mass is proportional to chiral condensate, it can be seen from Fig.1 that the larger the magnetic field is, the larger the corresponding chiral condensation is. This phenomenon is manifested as magnetic catalysis [19, 23, 24, 58], which accounts for the magnetic field has a strong tendency to enhance (or catalyze) spin-zero $\bar{q}q$ condensates.

By considering TSP of quarks, we investigate the temperature dependence of constituent quark mass for $eB = 0.05, 0.10, 0.15$ and 0.20 GeV^2 respectively shown in Fig.2(a, b). The dynamical mass M by considering TSP of quarks is manifested as a decreasing smooth function of temperatures for different magnetic fields and chemical potentials, which corresponds to a chiral crossover. The dynamical mass M is apparently enhanced with the increase of magnetic field, It is suggested that the introduction of TSP will enhance the magnetic catalysis effect.

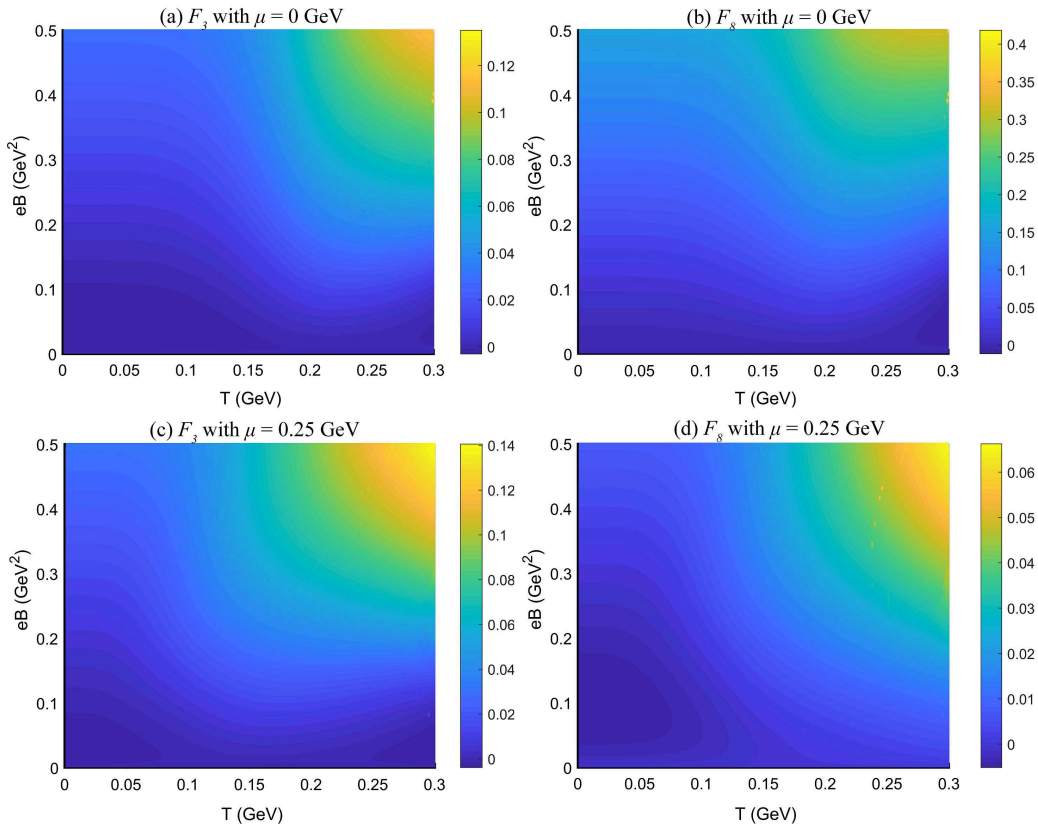


FIG. 3. Fig.3(a, b) shows the contour plots of the F_3 and F_8 distributions with zero chemical potential in the $T - eB$ plane, and Fig.3(c, d) shows similar plots of the F_3 and F_8 distributions but with non-zero chemical potential $\mu = 0.25 \text{ GeV}$.

In the $T - eB$ plane of the Fig.3, the corresponding temperature range is $0 \leq T \leq 0.3$ GeV, and the magnetic field range is $0 \leq eB \leq 0.5$ GeV². Fig.3 (a, b) displays the contour plots of the F_3 and F_8 distributions with zero chemical potential in the $T - eB$ plane, and Fig.3 (c, d) shows similar plots of the F_3 and F_8 distributions but with non-zero chemical potential $\mu = 0.25$ GeV. The $(2 + 1)$ -flavor spin polarization is different from that of two flavor spin polarization because of an additional term $F_8 = -2G_t \langle \bar{\psi} \Sigma^3 \lambda_8 \psi \rangle$ associated with the λ_8 flavor generator.

The spin condensates affect dynamical quark masses and quark dispersion relation. It is found that the nonzero values of the two spin condensates F_3 and F_8 exist in the restored chiral symmetry phase with high temperature and large magnetic field, but F_3 and F_8 are almost zero in the chiral symmetry broken phase. We also noticed that F_8 decreases sharply with the increase of chemical potential, but F_3 changes slightly with the chemical potential.

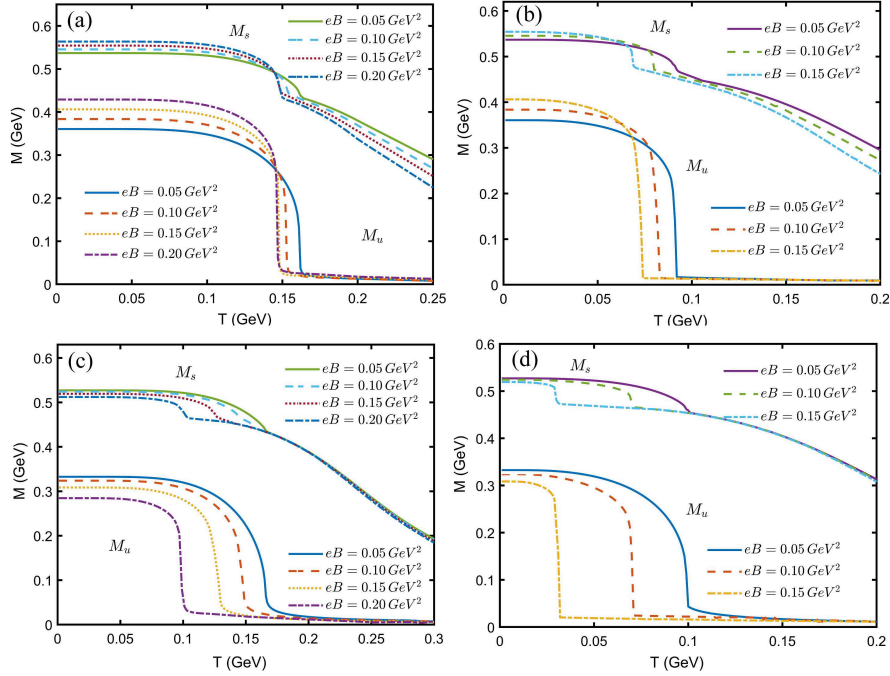


FIG. 4. The dynamical quark mass (M) as a function of temperature (T) for four different magnetic fields ($eB = 0.05, 0.10, 0.15$ and 0.20 GeV²) by considering the different sets of AMM. Fig.4(a, b) are for $\mu = 0$ and $\mu = 0.25$ GeV respectively with AMM1 set as $\kappa_u = \kappa_d = 0.38, \kappa_s = 0.25$. Fig.4(c, d) is same as Fig.4 (a, b) but for AMM2 set as $\kappa_u = 0.123, \kappa_d = 0.555, \kappa_s = 0.329$.

Figure 4. displays the dependence of dynamical quark mass (M) on temperature (T)

for four different magnetic fields ($eB = 0.05, 0.10, 0.15$ and 0.20 GeV^2) by considering the two AMM's sets. Fig.4(a, b) are for $\mu = 0 \text{ GeV}$ and $\mu = 0.25 \text{ GeV}$ with AMM1 set as $\kappa_u = \kappa_d = 0.38$ and $\kappa_s = 0.25$. Fig.4(c, d) is same as Fig.4(a, b) but with AMM2 set as $\kappa_u = 0.123, \kappa_d = 0.555$ and $\kappa_s = 0.329$. Contrary to the behavior of the zero AMM in Fig.1, the mass-decreasing behavior of u and d quarks in the chiral restoration is not a smooth slope but a sudden drop, which indicates the existence of a first-order transition. However, the smooth slope of the dynamical mass for the crossover can be still present in the weak field $eB = 0.05 \text{ GeV}^2$ for the non-zero AMM. The mass-decreasing behavior of s quark in the chiral restoration is still a smooth slope, which suggests a chiral crossover for s quark. From Fig.4, it is found that the dynamical quark mass of u and d quarks have the characteristics of inverse magnetic catalysis in the chiral restoration phase ($T \geq T_C$) by using the AMM sets.

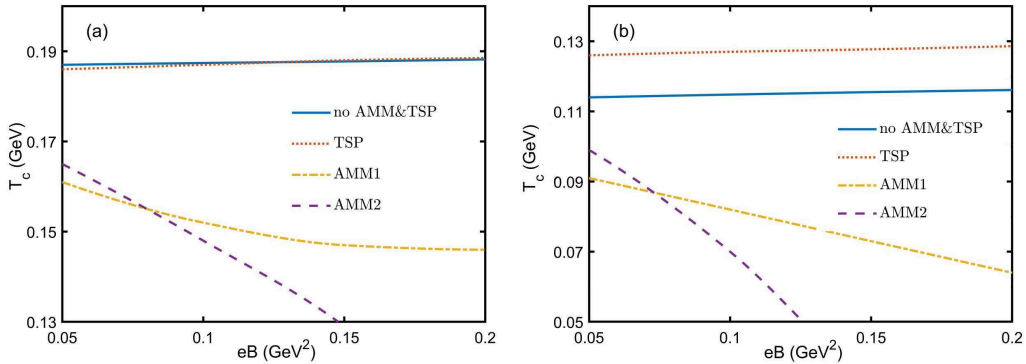


FIG. 5. The critical temperature of u and d quarks as a function of the magnetic field at $\mu = 0$ (a) and $= 0.25 \text{ GeV}$ (b).

In Fig. 5, the critical temperature is shown as a function of the magnetic field with the chemical potentials $\mu = 0$ and 0.25 GeV respectively. It is found that the critical temperature decreases with the magnetic field for the AMM1 and AMM2 sets, which indicates an inverse magnetic catalysis which qualitatively agrees with lattice result in [33].

On the contrary, with the TSP, T_C enhances as a function of the magnetic field, which is the extension of the magnetic catalysis effect from vacuum to finite temperature. The different effects of AMM and TSP on chiral condensate can be easily understood from the dispersion relations in Eq. (7) and Eq. (17), the AMM reduces the LLL energy and the TSP lifts up the LLL energy, which causes the different effects.

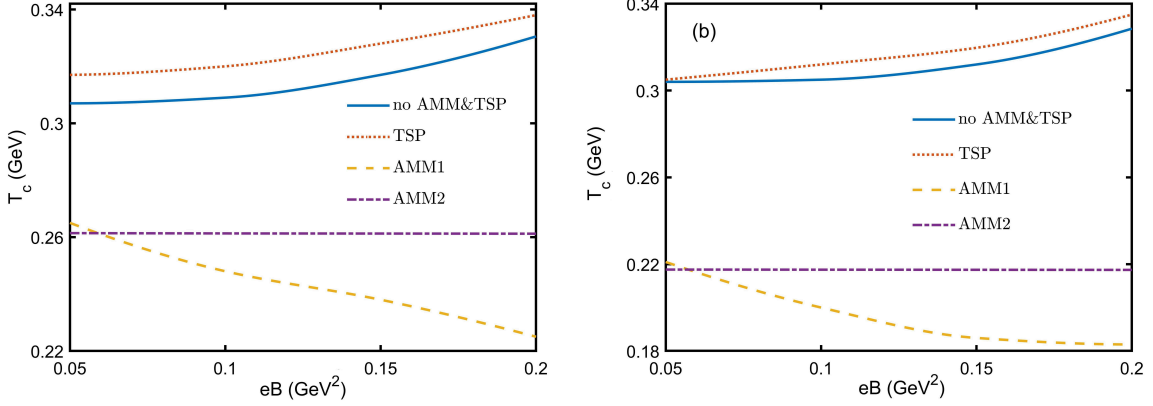


FIG. 6. The same as Fig. 5, but for the s -quark.

The critical temperature of chiral phase transition of s quark as a function of eB is manifested in Fig.6. Compared with light quarks of u and d , the phase transition temperature T_C of s quark with TSP increases significantly with the increase of magnetic field, which corresponds to the characteristics of magnetic catalysis. The introduction of AMM sets corresponds to inverse magnetic catalytic characteristics.

Figure 7 displays the dependencies of the entropy density of u , d and s quarks on temperature at zero chemical potential. It can be noted that the introduction of the AMM makes the crossover phase transition sharp. It is worth noting that the AMM in Fig.7 corresponds to three different settings, which are AMM0, AMM1 and AMM2, respectively. AMM0 means that the AMM is not considered, that is, all κ values in Eq. (17) are set to zero. AMM1 and AMM2 sets have been mentioned above. When $eB = 0.05 \text{ GeV}^2$, the magnetic field is not big enough to excite the effect on entropy. When $eB = 0.2 \text{ GeV}^2$, some of the effects of the magnetic field on entropy for different AMM sets and TSP can be excited. It is found that the entropy shows a sharp change near the phase transition temperature after adding AMM sets, and this sharp change is more obvious with the magnetic field increases and chemical potential, showing a first-order phase characteristic. The change of entropy with temperature near the phase transition temperature is relatively smooth after adding TSP, and it behaves like the crossover transition.

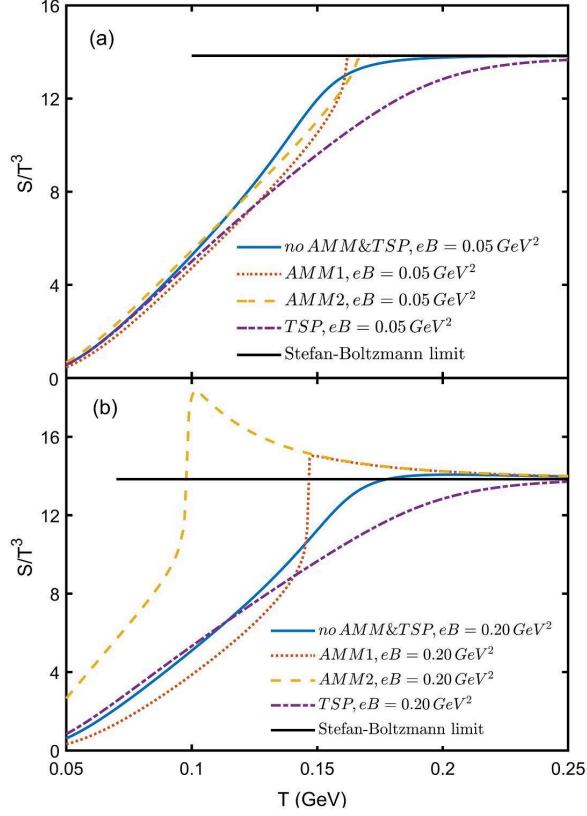


FIG. 7. The dependence of S/T^3 on temperature T at $\mu = 0\text{GeV}$ with different magnetic field. Fig.7 (a) is for $eB = 0.05 \text{ GeV}^2$ and Fig.7 (b) is for $eB = 0.2 \text{ GeV}^2$.

The dependence of square of sound-velocity c_s^2 on temperature T is manifested in Fig.8. Fig.8(a) and Fig.8(b) are for zero chemical potential $\mu = 0$ and $\mu = 0.25 \text{ GeV}$ respectively. The square of sound-velocity shows a sudden rapid rise inflection near the phase transition after adding AMM sets, and this rapid rise is more obvious with the magnetic field increases, showing a obviously first-order phase characteristic. On the other hands, the change of square of sound-velocity with temperature near the phase transition is relatively smooth inflection after adding TSP, showing a obviously cross-over transition characteristic. The result obtained by using the square of sound velocity is completely consistent with the result of entropy analysis.

Compared with u and d quarks, the square of sound-velocity of s quark with temperature is relatively smooth inflection after adding TSP and AMM sets. It is proposed that s quarks have always maintained obvious cross-over characteristics. In the high-temperature region, the square of sound-velocity c_s^2 increases with temperature and obtains the saturation value

$c_s^2 = 1/3$ to satisfy the relativistic requirement. This suggests that the equation of state in the chiral restoration phase at high temperatures is close to the Stefan-Boltzmann limit $\varepsilon = 3P$.

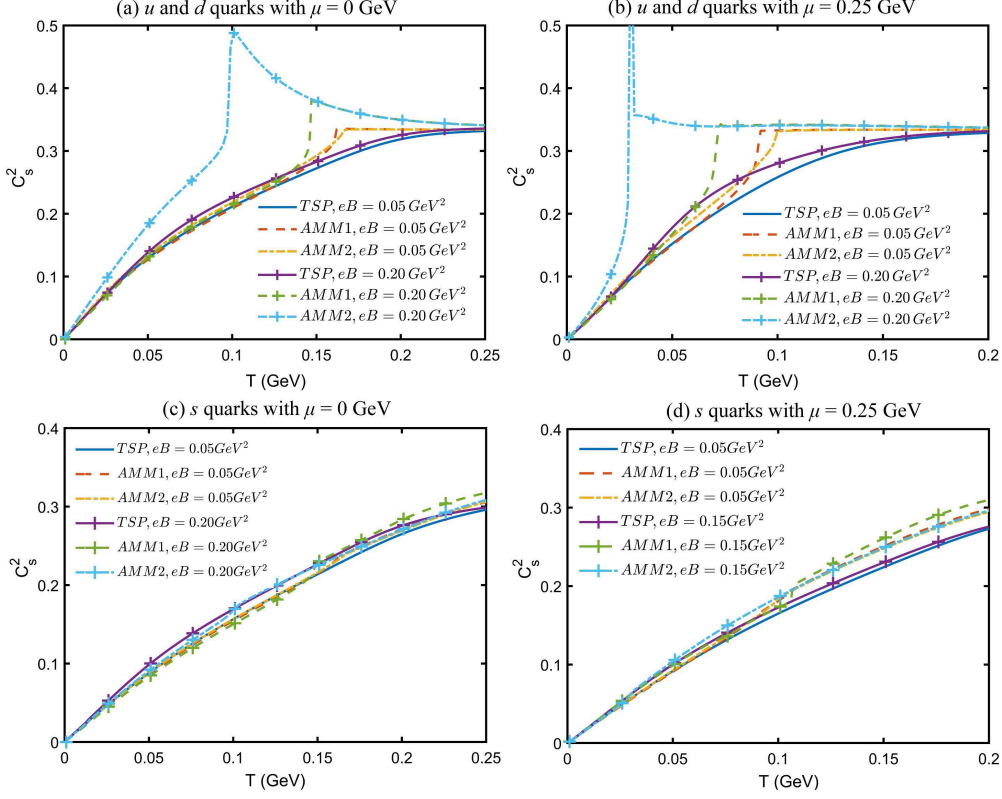


FIG. 8. The sound-velocity square C_s^2 of u and d with s quarks as a function of the temperature T with different chemical potential. Fig.8 (a, b) is for u and d quarks with zero chemical potential $\mu = 0$, and $\mu = 0.25$ GeV, and Fig.8 (c, d) is for s quarks

IV. SUMMARY AND CONCLUSIONS

In this work, we thoroughly study the effect from TSP and AMM on the vacuum, phase transition and thermal magnetized QCD in the $(2 + 1)$ -flavor Nambu-Jona-Lasinio (NJL) model with nonzero current quark masses at finite temperature and chemical potential. An unified physical mechanism to illustrate the novel consequences from recent lattice QCD as magnetic catalysis and inverse magnetic catalysis effect proposed in the paper.

We focus on two topics: the AMM and TSP. For these two topics, we should pay special attention to the dispersion relation, especially the lowest Landau level, which determines

the properties of the magnetized quark matter system. The TSP lifts up the LLL energy: $E_{\text{LLL}} = \left(p_z^2 + \left(M + F_3 + \frac{F_8}{\sqrt{3}} \right)^2 \right)^{\frac{1}{2}}$, while the AMM effect diminishes the LLL energy: $E_{\text{LLL}} = \left(p_z^2 + (M - \kappa |q_f| B)^2 \right)^{1/2}$ therefore, the TSP and the AMM take almost opposite effects on magnetized quark matter. When the AMM and TSP contributions are not considered, the corresponding phase transition temperature increases with the magnetic field, showing the characteristics of magnetic catalysis. When considering only the contribution of TSP, the phase transition temperature also increases with the magnetic field, showing the characteristics of magnetic catalysis. On the other hand, when AMM are introduced, the phase transition temperature decreases with the magnetic field, showing the characteristics of inverse magnetic catalysis.

It is found that the square of sound-velocity shows a sudden rapid rise inflection near the phase transition after adding AMM sets, and this rapid rise is more obvious with the magnetic field increases, showing a obviously first-order phase characteristic. On the other hands, after adding TSP, the change of square of sound-velocity with temperature near the phase transition is relatively smooth inflection, showing a obviously cross-over transition characteristic. The result obtained by using the square of sound velocity is completely consistent with the result of entropy analysis.

The $(2 + 1)$ -flavor spin polarization is different from that of two flavor because of an additional $F_8 = -2G_t \langle \bar{\psi} \Sigma^3 \lambda_8 \psi \rangle$ associated with the λ_8 flavor generator. The spin condensates affect the dynamical quark masses, chiral phase transition, and quark dispersion relation. It is found that the nonzero values of the two spin condensates F_3 and F_8 exist in the restored chiral symmetry phase with high temperature and large magnetic field, but F_3 and F_8 are almost zero in the chiral symmetry broken phase.

ACKNOWLEDGMENTS

This work was supported by National Natural Science Foundation of China (Grants No. 11875178, No. 11475068, No. 11747115).

REFERENCES

- [1] T. Vachaspati, *Phys. Lett. B* **265**, 258 (1991).
- [2] V. Skokov, A. Y. Illarionov, and V. Toneev, *Int. J. Mod. Phys. A* **24**, 5925 (2009).
- [3] W.-T. Deng and X.-G. Huang, *Phys. Rev. C* **85**, 044907 (2012).
- [4] Y.-J. Mo, S.-Q. Feng, and Y.-F. Shi, *Phys. Rev. C* **88**, 024901 (2013).
- [5] Y. Zhong, C.-B. Yang, X. Cai, and S.-Q. Feng, *Adv. High Energy Phys.* **2014**, 193039 (2014).
- [6] K. Kiuchi, P. Cerdá-Durán, K. Kyutoku, Y. Sekiguchi, and M. Shibata, *Phys. Rev. D* **92**, 124034 (2015).
- [7] L. Baiotti and L. Rezzolla, *Rept. Prog. Phys.* **80**, 096901 (2017).
- [8] T. Tatsumi, *AIP Conf. Proc.* **847**, 171 (2006).
- [9] R. C. Duncan and C. Thompson, *Astrophys. J. Lett.* **392**, L9 (1992).
- [10] A. Bzdak, S. Esumi, V. Koch, J. Liao, M. Stephanov, and N. Xu, *Phys. Rept.* **853**, 1 (2020).
- [11] D. E. Kharzeev, J. Liao, S. A. Voloshin, and G. Wang, *Prog. Part. Nucl. Phys.* **88**, 1 (2016).
- [12] X.-G. Huang, *Rept. Prog. Phys.* **79**, 076302 (2016).
- [13] J. O. Andersen, W. R. Naylor, and A. Tranberg, *Rev. Mod. Phys.* **88**, 025001 (2016).
- [14] V. A. Miransky and I. A. Shovkovy, *Phys. Rept.* **576**, 1 (2015).
- [15] U. Gürsoy, D. Kharzeev, and K. Rajagopal, *Phys. Rev. C* **89**, 054905 (2014).
- [16] D. She, S.-Q. Feng, Y. Zhong, and Z.-B. Yin, *Eur. Phys. J. A* **54**, 48 (2018).
- [17] B.-X. Chen and S.-Q. Feng, *Chin. Phys. C* **44**, 024104 (2020).
- [18] X. Chen, S.-Q. Feng, Y.-F. Shi, and Y. Zhong, *Phys. Rev. D* **97**, 066015 (2018).
- [19] D. E. Kharzeev, L. D. McLerran, and H. J. Warringa, *Nucl. Phys. A* **803**, 227 (2008).
- [20] K. Fukushima, D. E. Kharzeev, and H. J. Warringa, *Phys. Rev. D* **78**, 074033 (2008).
- [21] Y. Guo, S. Shi, S. Feng, and J. Liao, *Phys. Lett. B* **798**, 134929 (2019).
- [22] J. Deng and S.-Q. Feng, *Phys. Rev. D* **105**, 026015 (2022).
- [23] V. P. Gusynin, V. A. Miransky, and I. A. Shovkovy, *Nucl. Phys. B* **563**, 361 (1999).
- [24] V. P. Gusynin, V. A. Miransky, and I. A. Shovkovy, *Nucl. Phys. B* **462**, 249 (1996).
- [25] S. P. Klevansky and R. H. Lemmer, *Phys. Rev. D* **39**, 3478 (1989).
- [26] G. S. Bali, F. Bruckmann, G. Endrodi, F. Gruber, and A. Schaefer, *JHEP* **04**, 130 (2013).

- [27] G. S. Bali, F. Bruckmann, G. Endrodi, Z. Fodor, S. D. Katz, and A. Schafer, [Phys. Rev. D **86**, 071502 \(2012\)](#).
- [28] G. S. Bali, F. Bruckmann, G. Endrodi, Z. Fodor, S. D. Katz, S. Krieg, A. Schafer, and K. K. Szabo, [JHEP **02**, 044 \(2012\)](#).
- [29] M. D’Elia, F. Manigrasso, F. Negro, and F. Sanfilippo, [Phys. Rev. D **98**, 054509 \(2018\)](#).
- [30] E. J. Ferrer, V. de la Incera, I. Portillo, and M. Quiroz, [Phys. Rev. D **89**, 085034 \(2014\)](#).
- [31] E. J. Ferrer, V. de la Incera, and X. J. Wen, [Phys. Rev. D **91**, 054006 \(2015\)](#).
- [32] J. Chao, P. Chu, and M. Huang, [Phys. Rev. D **88**, 054009 \(2013\)](#).
- [33] G. S. Bali, F. Bruckmann, M. Constantinou, M. Costa, G. Endrodi, S. D. Katz, H. Panagopoulos, and A. Schafer, [Phys. Rev. D **86**, 094512 \(2012\)](#).
- [34] G. S. Bali, G. Endrődi, and S. Piemonte, [JHEP **07**, 183 \(2020\)](#).
- [35] S. Fayazbakhsh and N. Sadooghi, [Phys. Rev. D **90**, 105030 \(2014\)](#).
- [36] E. J. Ferrer, V. de la Incera, D. Manreza Paret, A. Pérez Martínez, and A. Sanchez, [Phys. Rev. D **91**, 085041 \(2015\)](#).
- [37] N. Chaudhuri, S. Ghosh, S. Sarkar, and P. Roy, [Phys. Rev. D **99**, 116025 \(2019\)](#).
- [38] S. Ghosh, N. Chaudhuri, S. Sarkar, and P. Roy, [Phys. Rev. D **101**, 096002 \(2020\)](#).
- [39] N. Chaudhuri, S. Ghosh, S. Sarkar, and P. Roy, [Eur. Phys. J. A **56**, 213 \(2020\)](#).
- [40] S. Mao and D. H. Rischke, [Phys. Lett. B **792**, 149 \(2019\)](#).
- [41] J. Mei and S. Mao, [Phys. Rev. D **102**, 114035 \(2020\)](#).
- [42] E. J. Ferrer and V. de la Incera, [Nucl. Phys. B **824**, 217 \(2010\)](#).
- [43] L. Chang, Y.-X. Liu, and C. D. Roberts, [Phys. Rev. Lett. **106**, 072001 \(2011\)](#).
- [44] E. J. Ferrer and V. de la Incera, [Phys. Rev. Lett. **102**, 050402 \(2009\)](#).
- [45] F. Preis, A. Rebhan, and A. Schmitt, [JHEP **03**, 033 \(2011\)](#).
- [46] P. J. A. Bicudo, J. E. F. T. Ribeiro, and R. Fernandes, [Phys. Rev. C **59**, 1107 \(1999\)](#).
- [47] K. Xu, J. Chao, and M. Huang, [Phys. Rev. D **103**, 076015 \(2021\)](#).
- [48] M. Buballa, [Phys. Rept. **407**, 205 \(2005\)](#).
- [49] T. Hatsuda and T. Kunihiro, [Phys. Rept. **247**, 221 \(1994\)](#).
- [50] U. Vogl and W. Weise, [Prog. Part. Nucl. Phys. **27**, 195 \(1991\)](#).
- [51] P. Rehberg, S. P. Klevansky, and J. Hufner, [Phys. Rev. C **53**, 410 \(1996\)](#).
- [52] F. Lin, K. Xu, and M. Huang, [Phys. Rev. D **106**, 016005 \(2022\)](#).
- [53] H. Kohyama, D. Kimura, and T. Inagaki, [Nucl. Phys. B **906**, 524 \(2016\)](#).

- [54] M. Mekhfi, [Phys. Rev. D **72**, 114014 \(2005\)](#).
- [55] Y. Dothan, [Physica A **114**, 216 \(1982\)](#).
- [56] D. P. Menezes, M. Benghi Pinto, S. S. Avancini, A. Perez Martinez, and C. Providencia, [Phys. Rev. C **79**, 035807 \(2009\)](#).
- [57] R. M. Aguirre, [Phys. Rev. D **102**, 096025 \(2020\)](#).
- [58] V. P. Gusynin, V. A. Miransky, and I. A. Shovkovy, [Phys. Rev. Lett. **73**, 3499 \(1994\)](#).